HAL
open science

Probing the activity of diguanylate cyclases and c-di-GMP phosphodiesterases in real-time by CD spectroscopy.

Valentina Stelitano, Annegret Brandt, Silvia Fernicola, Stefano Franceschini, Giorgio Giardina, Andrea Pica, Serena Rinaldo, Filomena Sica, Francesca Cutruzzolà

To cite this version:

Valentina Stelitano, Annegret Brandt, Silvia Fernicola, Stefano Franceschini, Giorgio Giardina, et al.. Probing the activity of diguanylate cyclases and c-di-GMP phosphodiesterases in real-time by CD spectroscopy.. Nucleic Acids Research, 2013, 41 (7), pp.e79. 10.1093/nar/gkt028 . pasteur-01048743

HAL Id: pasteur-01048743

https://riip.hal.science/pasteur-01048743v1

Submitted on 25 Jul 2014

HAL is a multi-disciplinary open access archive for the deposit and dissemination of scientific research documents, whether they are published or not. The documents may come from teaching and research institutions in France or abroad, or from public or private research centers.

L'archive ouverte pluridisciplinaire **HAL**, est destinée au dépôt et à la diffusion de documents scientifiques de niveau recherche, publiés ou non, émanant des établissements d'enseignement et de recherche français ou étrangers, des laboratoires publics ou privés.

Published online 28 January 2013 Nucleic Acids Research, 2013, Vol. 41, No. 7 e79
doi:10.1093/nar/gkt028

Probing the activity of diguanylate cyclases and c-di-GMP phosphodiesterases in real-time by CD spectroscopy

Valentina Stelitano[1], Annegret Brandt[1], Silvia Fernicola[1], Stefano Franceschini[1], Giorgio Giardina[1], Andrea Pica[2], Serena Rinaldo[1], Filomena Sica[2,3] and Francesca Cutruzzolà[1,*]

[1]Istituto Pasteur-Fondazione Cenci Bolognetti, Department of Biochemical Sciences, Sapienza University of Rome, 00185 Rome, Italy, [2]Department of Chemical Sciences, University of Naples 'Federico II', 80126 Naples, Italy and [3]Institute of Biostructure and Bioimaging, CNR, 80134 Naples, Italy

Received September 27, 2012; Revised December 7, 2012; Accepted January 3, 2013

ABSTRACT

Bacteria react to adverse environmental stimuli by clustering into organized communities called biofilms. A remarkably sophisticated control system based on the dinucleotide 3′–5′ cyclic diguanylic acid (c-di-GMP) is involved in deciding whether to form or abandon biofilms. The ability of c-di-GMP to form self-intercalated dimers is also thought to play a role in this complex regulation. A great advantage in the quest of elucidating the catalytic properties of the enzymes involved in c-di-GMP turnover (diguanylate cyclases and phosphodiesterases) would come from the availability of an experimental approach for *in vitro* quantification of c-di-GMP in real-time. Here, we show that c-di-GMP can be detected and quantified by circular dichroism (CD) spectroscopy in the low micromolar range. The method is based on the selective ability of manganese ions to induce formation of the intercalated dimer of the c-di-GMP dinucleotide in solution, which displays an intense sigmoidal CD spectrum in the near-ultraviolet region. This characteristic spectrum originates from the stacking interaction of the four mutually intercalated guanines, as it is absent in the other cyclic dinucleotide 3′–5′ cyclic adenilic acid (c-di-AMP). Thus, near-ultraviolet CD can be used to effectively quantify in real-time the activity of diguanylate cyclases and phosphodiesterases in solution.

INTRODUCTION

The bacterial signaling molecule 3′–5′ cyclic diguanylic acid (c-di-GMP) (Figure 1) has recently attracted growing interest because of its central role in modulation of several cellular processes, including biofilm formation and drug resistance (1–3). The intracellular levels of c-di-GMP are modulated by the opposite activity of diguanylate cyclases (DGCs), which catalyze its synthesis from two GTP molecules, and specific phosphodiesterases (PDEs), which hydrolyze it into linear 5′-phosphoguanylyl-(3′–5′)-guanosine (pGpG) or to two molecules of GMP. The central role of these enzymes in biofilm formation makes them an ideal target for the development of new anti-biofilm compounds. It is known that c-di-GMP displays a rich polymorphism in solution, and that the equilibrium among the monomeric, dimeric, tetrameric and octameric species is affected by the presence of metal ions (4–6). However, only the monomeric and dimeric forms (Figure 1) have been found under physiological conditions, whereas higher oligomer formation occurs only at mM concentration or in presence of additional aromatic intercalators (7,8). The monomer–dimer equilibrium is also likely to play a physiological role, allowing bacteria to sense and control different local c-di-GMP concentrations. Indeed PilZ receptors binding to c-di-GMP as a monomer or as an intercalated dimer have been reported (9–11). The dimeric form is also observed in complex with DGCs, bound to a non-competitive inhibitory site (12–14), whereas PDEs bind c-di-GMP as a monomer at the active site (15–17). Despite the great effort in understanding the molecular

*To whom correspondence should be addressed. Tel: +39 06 49910955; Fax: +39 06 4440062; Email: francesca.cutruzzola@uniroma1.it

The authors wish it to be known that, in their opinion, the first two authors should be regarded as joint First Authors.

© The Author(s) 2013. Published by Oxford University Press.
This is an Open Access article distributed under the terms of the Creative Commons Attribution Non-Commercial License (http://creativecommons.org/licenses/by-nc/3.0/), which permits unrestricted non-commercial use, distribution, and reproduction in any medium, provided the original work is properly cited.

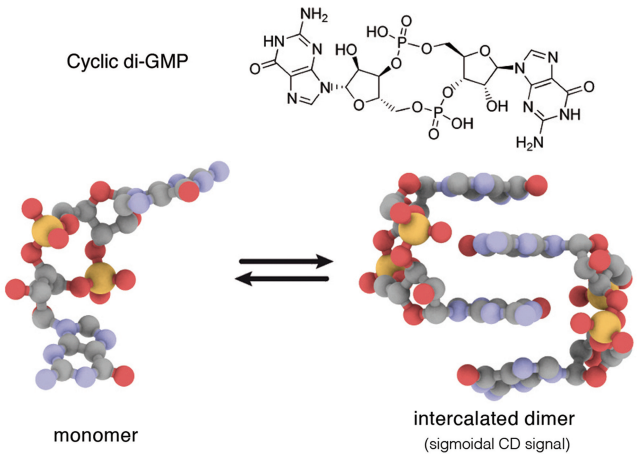

Figure 1. Chemical structure of c-di-GMP and 3D structure of monomeric and dimeric c-di-GMP as observed in the active and inhibitory site of PleD, respectively (PDB ID: 1w25) (14). The equilibrium in solution of the two species is affected by the presence of monovalent or divalent cations (4–6).

basis of the c-di-GMP signaling pathways and the growing number of groups working in this field, a method for *in vitro* detection and quantification of c-di-GMP produced or degraded by DGCs and PDEs is still not available for reliable real-time measurements. The direct and indirect methods currently available for c-di-GMP quantification in enzymatic reactions are summarized in Table 1, together with the enzyme(s) whose kinetic activity has been characterized to date using the various methods.

Here, we report the detection and quantification of c-di-GMP in solution by circular dichroism (CD) spectroscopy, a technique routinely used in protein and nucleic acids characterization. This method is based on the ability of manganese ions to promote c-di-GMP dimerization, giving rise to an intense CD signal because of the hyperchromic effect of the four stacked bases. The CD signal linearly depends on c-di-GMP concentration (even in the low micromolar range). The crystallographic structure of the c-di-GMP–manganese complex was also solved and compared with that of the complex with magnesium, previously available (36). The CD method presented here, which does not require the addition of chromophores, can be easily applied to measure the kinetics of enzymes involved in c-di-GMP turnover (DGCs and PDEs) in real-time, as supported by the results reported in this work on two model enzymes (PleD and RocR). To allow a better comparative evaluation, we have also highlighted similarities and differences of this method with other techniques available to date. Given that we are only starting to appreciate the extent to which DGCs and PDEs domain-containing proteins are functionally diversified in bacteria, the availability of a novel biochemical method able to measure both the DGC and PDE activity in detail can be strategic in the c-di-GMP field.

MATERIALS AND METHODS

General methods

CD experiments were carried out using quartz cuvettes (Hellma) with a path length of 1 cm on a JASCO J-710 spectropolarimeter. Spectra were baseline corrected by subtracting the buffer from the raw data, and the signal was adjusted to zero at 340 nm, as no optical activity is expected at this wavelength. High-performance liquid chromatography (HPLC) analysis was performed on a 150- × 4.6-mm reverse phase column (Prevail C8, Grace Davison Discovery Science) at room temperature on a LabFlow 4000 apparatus (LabService Analytica). Detection wavelength was 252 nm, and mobile phase was 100 mM phosphate buffer pH 5.8/methanol (98/2, v/v).

Influence of metal ions on c-di-GMP

To verify the influence of metal ions on the c-di-GMP dimer formation, samples containing 15 μM c-di-GMP (Biolog) in 20 mM Tris, pH 8, and 100 mM NaCl were analyzed in the presence of 2.5–10 mM of manganese and/or magnesium chloride. To obtain the calibration curves, increasing concentrations of c-di-GMP (1, 5, 10, 15, 20, 25 and 30 μM) in 20 mM Tris, pH 8, 100 mM NaCl, 10 mM $MgCl_2$, 1 mM $BeCl_2$, 10 mM NaF and 2.5 mM $MnCl_2$ (reaction buffer of PleD) were analyzed. The same profile is obtained in the absence of BeF_2 (data not shown). CD analysis was performed in duplicates at 10°C, 25°C and 37°C.

Analysis of manganese affinity for c-di-GMP

Increasing concentrations of $MnCl_2$ (0.2–15 mM) were added to a sample containing 15 μM c-di-GMP (Biolog) in 50 mM Tris, pH 7.5, 150 mM NaCl and 10 mM $MgCl_2$. CD spectra were recorded at 10°C after allowing the samples to equilibrate for 10 min. A K_D of 262 ± 36 μM for the c-di-GMP-Mn^{2+} complex was calculated by fitting the observed CD_{282} signal as a function of $MnCl_2$ concentration.

CD spectra of other nucleotides

The CD spectra of 15 μM pGpG (Biolog), c-di-GMP, GMP (Sigma Aldrich) and GTP (Amersham Bioscience) and c-di-AMP (Biolog) were recorded in 50 mM Tris, pH 8, 150 mM NaCl, 10 mM $MgCl_2$ and 2.5 mM $MnCl_2$. The spectra vary slightly with buffer conditions. The concentration of stock solutions of GTP and GMP was determined by measuring the absorption at 253 nm using 13 700 $M^{-1}cm^{-1}$ and 13 300 $M^{-1}cm^{-1}$ as molar extinction coefficients.

Kinetic studies

To study the diguanylate cyclase activity of purified *Caulobacter crescentus* PleD, a 0.5 μM enzyme solution was incubated for 10 min at room temperature in 20 mM Tris, pH 8, 100 mM NaCl, 10 mM $MgCl_2$. The enzyme was then activated by adding 1 mM $BeCl_2$ and 10 mM NaF and kept at room temperature for 30 min. The diguanylate cyclase reaction was performed at 20°C in the presence of 2.5 mM $MnCl_2$ and was started by adding 100 μM GTP; the time course of the reaction was followed by directly measuring the CD signal at 282 nm. In parallel, the reaction was followed under the same experimental

Table 1. Analytical methods available to measure enzymatic c-di-GMP synthesis and degradation

Method	Real-time	Advantage	Disadvantage	Enzyme analyzed		References
				DGC	PDE[a]	
Circular dichroism	YES	Pre-steady and steady-state kinetics	Micromolar detection limit	PleD	RocR	Present work
Thin layer chromatography (alfa^{32}P-GTP or ^{33}P-C-di-GMP)	NO	Good sensitivity (<μM)	Radiolabeled precursors required Enzyme inactivation step required before analysis	PleD DosC[b] All2874[b]		(18–20) (21) (22)
					CC3396 PdeB (HD-GYP)	(23) (24)
ENZ.CHECK Pyrophosphate detection kit	YES (DGC)	Steady state kinetics	Only valid for DGCs Upper limit for PPi detection (5 μM/min)	WspR XCC4471		(13) (12)
Coupled colorimetric assay (monitors PPi production)			Susceptible of Pi contamination	PleD		(25)
Malachite Green Coupled colorimetric assay (monitors Pi production)	NO		Enzyme inactivation step required before analysis Susceptible of Pi contamination	PleD[b]		(14)
Reverse-phase HPLC Detection of nucleotides	NO	Nucleotides can be analyzed by mass spectrometry	Enzyme inactivation step required before analysis	WspR[b] PleD AnapPleD[b] HemDGC thermoDGC[b]		(13) (18) (26) (27) (28)
					RavR[b] RocR BlrP1 PA2567 PdeR RpfG (HD-GYP)	(29) (30) (31) (32) (33) (34)
DYE(S) BINDING to c-di-GMP quadruplex	NO		Only valid for DGCs Limited Dye solubility Enzyme inactivation step required before analysis Slow kinetics of complex formation	WspR		(7,8)
Fluorescence[c] (MANT-c-di-GMP)	YES (PDE)	Steady-state kinetics	Only valid for PDEs		MSDGC-1	(35)

[a]All c-di-GMP phosphodiesterases listed in the Table belong to the EAL-type PDEs, unless specifically indicated in brackets.
[b]Qualitative attribution of enzymatic activity: catalytic parameters were not determined in the corresponding publication.
[c]MANT = N-Methylisatoic anhydride.

conditions, but aliquots were taken at different times (1, 3, 5, 10, 30 and 60 min); samples were boiled for 10 min to stop the enzymatic reaction, spun down and filtered to remove the precipitated protein. The samples were then analyzed both by CD spectroscopy at 20°C and by Reverse-Phase-HPLC as described earlier in the text. The experiment was performed in duplicate. PleD was purified as previously described by Wassmann *et al.* (25). The enzymatic activity of beryllium-activated PleD was found to be 20 nmol/min/mg, in good agreement with the value previously published (18,19).

To study the phosphodiesterase activity of *Pseudomonas aeruginosa* RocR, a 0.5 μM enzyme solution was incubated for 10 min at room temperature in 20 mM Tris, pH 8, 100 mM NaCl, 5 mM $MgCl_2$ and 2.5 mM $MnCl_2$. The reaction was performed at 20°C and was started by adding 30 μM c-di-GMP. The enzymatic reaction was followed in real-time at 282 nm. In parallel, aliquots were taken at different times (3, 5, 15, 30 and 45 min), and 100 mM $CaCl_2$ or 25 mM ethylenediaminetetraacetic acid, pH 6.0, was added to stop the enzymatic reaction; samples were boiled for 10 min, spun down and filtered to remove the precipitated protein. Samples were then analyzed by CD spectroscopy at 20°C and by Reverse-Phase-HPLC. The experiment was performed in duplicate. RocR was purified as previously described by De *et al.* (13). The turnover number of RocR was found to be 0.1 s^{-1}, somewhat slower than the value previously published (0.67 s^{-1}), in which the activity was measured by following the production of pGpG at 23°C in the presence of 25 mM $MgCl_2$ (30); this difference is not surprising given the different experimental conditions used in the present work (lower temperature and $MgCl_2$ concentration).

Titration of PleD with c-di-GMP

To study the binding of c-di-GMP to PleD, increasing concentrations of c-di-GMP were added to a sample containing 10 μM of PleD in 20 mM Tris, pH 8, 100 mM NaCl, 10 mM $MgCl_2$, 1 mM $BeCl_2$ and 10 mM NaF. CD spectra were taken at 25°C after equilibration of the system. The spectra of the samples containing 25, 30, 35 and 40 μM c-di-GMP were measured again after the addition of $MnCl_2$ to a final concentration of 2.5 mM. The order of addition of the three components in the mixture (i.e. PleD + c-di-GMP + Mn^{2+} or c-di-GMP + PleD + Mn^{2+} or c-di-GMP + Mn^{2+} + PleD) did not change the final spectrum (data not shown). The experiment was performed in triplicate.

Crystallization, data collection and structure solution

Single crystals of $[Mn(H_2O)_4(c\text{-di-GMP})_2]^{2+}$ complex suitable for X-ray diffraction were obtained by hanging drop vapor diffusion method. The best diffracting crystals grew from drops of 6 μl, obtained by mixing 5 μl of c-di-GMP solution (c-di-GMP 4.3 mM; $MnCl_2$ 30 mM; cacodilate, pH 6.5, 50 mM) and 1 μl of reservoir solution (2-methyl-2,4-pentanediol 50% v/v; cacodilate, pH 6.5, 50 mM). A crystal ($0.5 \times 0.5 \times 0.2$ mm^3) was mounted at room temperature on a Bruker-Nonius Kappa CCD diffractometer equipped with a graphite monochromatedMoKα radiation (λ = 0.71073 Å, CCD rotation images). The crystal was tetragonal with space group $I4_1$ and unit cell parameters: a = b = 20.05, c = 39.55 Å. Semi-empirical absorption correction (SADABS) was applied. Fourier reflection pairs were not merged to consider anomalous scattering from manganese and phosphorous atoms. The structure was solved by direct methods [SIR97 package (37)] and refined by the full matrix least-squares method on F^2 against all independent measured reflections [SHELXL program of SHELX97 package (38)].

All non-hydrogen atoms were refined anisotropically. The final refinement converged to an R-value of 0.0969, for reflection with $I > 2\sigma(I)$. Twinning by merohedry [180° rotation about (1 1 0)] was detected and contemplated in the refinement (the calculated twinning fraction was 0.186). Crystal data and refinement details are summarized in Supplementary Table S1. CCDC 913765 contains the supplementary crystallographic data for this article. These data can be obtained free of charge at www.ccdc.cam.ac.uk/conts/retrieving.html or from the Cambridge Crystallographic Data Centre, 12 Union Road, Cambridge CB2 1EZ, UK; fax: (international) +44 1223/336 033.

RESULTS AND DISCUSSION

Formation of the complex between c-di-GMP and manganese

The method presented here is based on the specific CD signal displayed by the intercalated dimer of c-di-GMP and on the ability of manganese ions to promote dimerization of this cyclic dinucleotide. The CD profile of c-di-GMP shows two peaks in the absence of metal ions,

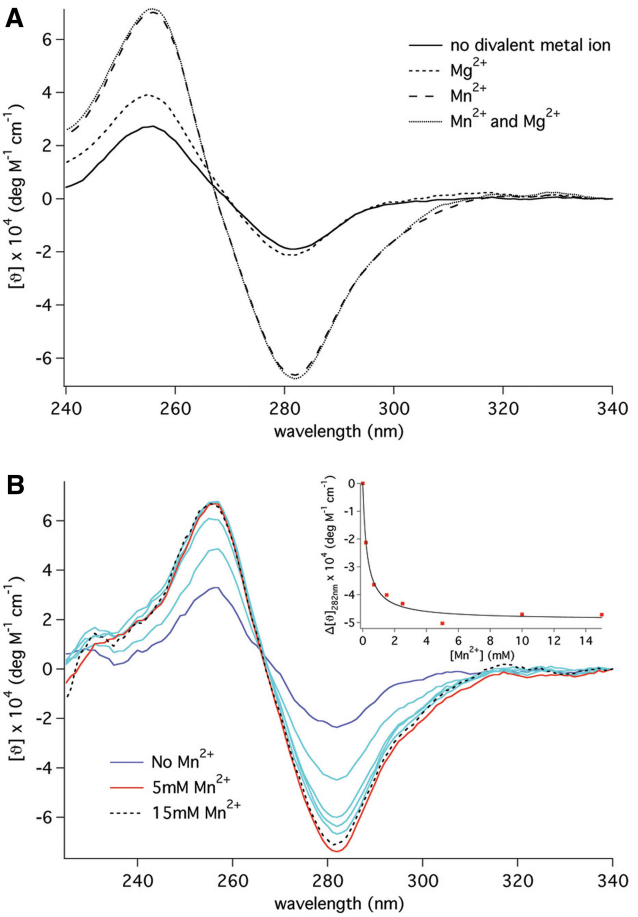

Figure 2. Effect of manganese on the dichroic signal of c-di-GMP in solution. (**A**) Influence of divalent metal ions on c-di-GMP dimer formation analyzed in 50 mM Tris–HCl, pH 7.5, 150 mM NaCl, at 10°C. $MnCl_2$ and $MgCl_2$ were added to a final concentration of 2.5 and 10 mM, respectively. (**B**) CD spectra of c-di-GMP showing the increase in the intensity of the dimer-specific peaks in the presence of increasing manganese concentrations, analyzed in 50 mM Tris–HCl, pH 7.5, 150 mM NaCl, at 10°C. (Inset) Plot of the CD signal at 282 nm as function of Mn^{2+} concentration. Ninety-five per cent of signal saturation is observed at 2.5 mM $MnCl_2$ (i.e. K_D for c-di-GMP-Mn^{2+} complex formation of 262 ± 36 μM). The signal is corrected for the Mn^{2+}-free signal.

one positive at 255 nm and one negative at 282 nm (Figure 2A), similarly to that of left-handed Z DNA and inverted relative to right handed DNA and RNA (5). A sigmoidal CD profile is obtained when two or more identical chromophores are in close proximity (39); in the case of c-di-GMP, which can form a stable dimer in solution, a strong hyperchromic effect is observed, as previously reported (5) because of the stacking of the four guanine rings. As divalent metal ions are known to shift the equilibrium towards the dimer (4,5), we have analyzed the c-di-GMP CD profile in the presence of Mn^{2+} and/or Mg^{2+}, which are normally added to the reaction buffer of DGCs and PDEs enzymatic assays. Surprisingly, while the influence of Mg^{2+} on the spectroscopic signal was not significative, we found that the intensity of both 255 and 282 nm peaks increases in the presence of Mn^{2+} (Figure 2A). This is because of the formation of a stable

complex between the intercalated dimer of c-di-GMP and the manganese hydrated cation. Titration of c-di-GMP with Mn^{2+} shows that the CD signal at 282 nm reaches a plateau for Mn^{2+} concentrations above 2.5 mM (Figure 2B, inset), suggesting that the complex is >95% populated above this threshold.

The different dichroic features of c-di-GMP in the presence of Mn^{2+} and Mg^{2+} were unexpected because of the similarity of many properties between the two cations. Only two structures of a c-di-GMP intercalated dimer were solved, in complex with Mg^{2+} or Co^{2+}, respectively, both in the early 90s (36,40). We have solved the crystal structure of c-di-GMP in complex with Mn^{2+} to establish whether this cation, compared with Mg^{2+} (36), may induce any conformational change in the structural organization of the complex that could account for the different ability of the two divalent cations to populate the complex in solution. The crystal structure of the complex $[Mn(H_2O)_4(c\text{-di-GMP})_2]^{2+}$, determined at 0.9 Å resolution, is shown in Figure 3 and further illustrated in Supplementary Figure S1, Supplementary Movie S1 and Supplementary Table S1.

The structure shows non-significant differences with respect to that of the c-di-GMP-Mg^{2+} complex (36), indicating that the substitution of manganese with magnesium does not interfere with the assembly of the intercalated dimeric structure nor with the binding mode of the metal ion. On the basis of these data, it seems reasonable to assign the different effect of Mn^{2+} and Mg^{2+} on the dichroic spectra of c-di-GMP to the presence of d-electrons in Mn^{2+}, which contribute to the electrostatic interactions between the cation and guanine bases (41). This interpretation is in agreement with the order of nucleotide-binding ability of divalent cations ($Mg^{2+} < Co^{2+} < Ni^{2+} < Mn^{2+} < Zn^{2+} < Cd^{2+} < Cu^{2+}$) deduced by empirical studies in the late 60s (42) and with quantum chemical calculations, which suggest that the different action of Mg^{2+} and Mn^{2+} towards nucleobases derives from the greater polarization and charge-transfer effects in the Mn^{2+} complexes (43,44). Finally, comparative studies of the guanine ligand-binding properties of Mn^{2+}, Zn^{2+}, Ni^{2+} and Mg^{2+} have demonstrated that the transition metals show higher affinity for the nucleobase N7. This could determine the stabilization of the complex in the presence of Mn^{2+} (41). Accordingly, an enhancement of the CD signal similar to that observed in the presence of Mn^{2+} was observed also in the presence of zinc and nickel divalent cations (data not shown).

The formation of the c-di-GMP-Mn^{2+} complex occurs rapidly, within 5 min at 10°C and within the mixing time at 25°C (data not shown). In the presence of 2.5 mM Mn^{2+}, the CD signal shows a linear dependence on c-di-GMP concentration; this linearity is maintained at the different temperatures analyzed (10°C, 25°C and 37°C) (Figure 4). The CD signal of the samples is stable for at least 4 h in the temperature range needed for enzymatic reactions (10°C–37°C) and is also reproducible after a 12 h storage at 4°C (data not shown), making this method adaptable to different protocols (i.e. from real-time detection to multiple analysis of many stored samples). The intense CD signature of the intercalated dimer is specific, thus c-di-GMP can be detected and quantified (even in the low micromolar range) in the presence of all the other nucleotides involved in c-di-GMP turnover. GTP and GMP are spectroscopically silent in the near-ultraviolet region, whereas pGpG displays a CD spectrum with a single band at 255 nm that possibly originates from the coupling of the two guanines, which are in close proximity (Figure 5). However, as it does not significantly contribute at 282 nm, the presence of pGpG does not hamper the quantification of c-di-GMP at 282 nm (Figure 5).

To assign the spectroscopic signature seen by CD to the stacking of the guanine bases, we have also measured the spectrum of another dinucleotide, i.e. 3′–5′ cyclic diadenilic acid (c-di-AMP): as shown in Figure 5, this dinucleotide shows a much lower intensity and a different profile in the presence of Mn ions with respect to c-di-GMP. The observation that c-di-AMP does not show the same spectroscopic signature of c-di-GMP strongly suggests that the sigmoidal CD signal arises from the stacking of the guanine bases. A comparison of the chemical structure of c-di-GMP and c-di-AMP highlights that the difference in the substituents in position N1 and the absence of the carbonyl group in the purine ring of c-di-AMP may disfavor the formation of a stacked dimer by c-di-AMP (see Supplementary Figure S2).

Probing the enzymatic activity of DGCs and PDEs

The CD method described here allows measuring c-di-GMP concentration in the working range typical of DGCs and PDEs enzymes. We have used the CD analysis to measure the enzymatic activity of two reference enzymes, i.e. PleD, a well characterized DGC from *C. crescentus* and RocR from *P. aeruginosa*, an EAL-type PDE (18,30).

The time course of the reactions catalyzed by these two enzymes was measured in real-time at 282 nm as shown in Figure 6 (panels A and B, respectively). The reaction rates were found to be in good agreement with the published values (18,19,30) (see 'Materials and Methods' section). As a control, the time course was also measured by extracting the nucleotides from aliquots of the reaction mixture taken at given times; these aliquots were then analyzed in parallel both by CD spectroscopy and by reverse-phase HPLC chromatography, the most common method to quantify c-di-GMP (see also Table 1) (45). The results obtained by CD analysis (point measurements) are fully consistent with data obtained by reverse-phase HPLC. The comparison of the kinetics as followed by real-time measurements with that obtained by point measurements (see Figure 6) clearly shows (more evidently in the case of RocR) that the real-time approach is an absolute requirement for an accurate determination of the time course of the reaction. The time course of the reaction of RocR was also measured in the absence of Mn^{2+} (with Mg^{2+} ions alone), and no difference was observed in the kinetic parameters (data not shown), suggesting that the real-time measurement can be carried out,

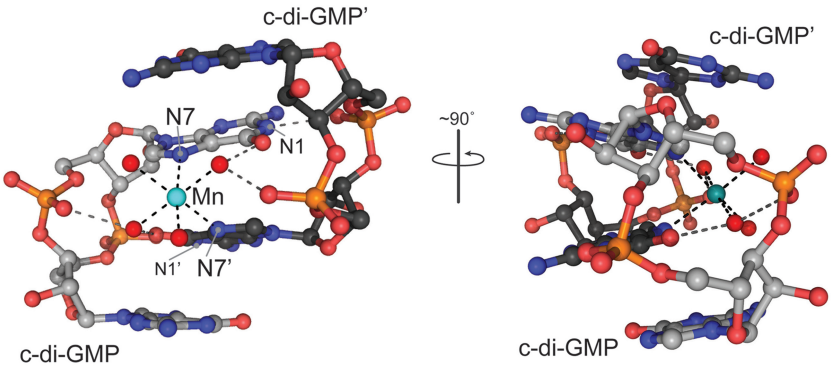

Figure 3. Structure of the $[Mn(H_2O)_4(c\text{-di-GMP})_2]^{2+}$ complex. Two c-di-GMP molecules (c-di-GMP and c-di-GMP') are kept together by a manganese ion (cyan), which is six-coordinated by four water molecules (red) and by the N7 and N7′ nitrogen atoms of guanines belonging to two different molecules. Each of the two axial water molecules is H-bonded to the carbonyl of one central guanine and to the oxygen of the cognate phosphate. The central base N1 of each molecule is hydrogen-bonded to the sugar phosphate backbone of the other. G–G base pairing interactions stabilize both the dinucleotides and the overall assembly. Finally, the guanine rings coordinated to Mn^{2+} are forced out of the ideal co-planarity and seem partially unstacked similarly to the central bases of the complex with Mg^{2+} (36). The crystallographic structure of the complex is further illustrated in Supplementary Figure S1 and Supplementary Movie S1.

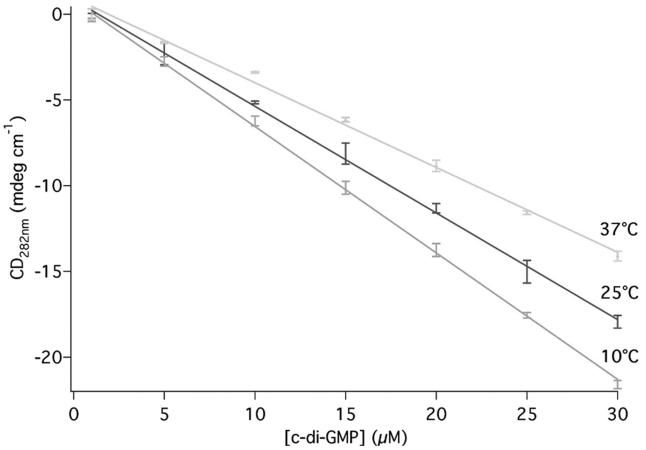

Figure 4. Linear dependence of the CD signal on c-di-GMP concentration. Analysis was performed at three different temperatures, i.e. 10°C, 25°C and 37°C, in the following buffer: 20 mM Tris–HCl, pH 8, 100 mM NaCl, 10 mM $MgCl_2$, 1 mM $BeCl_2$, 10 mM NaF and 2.5 mM $MnCl_2$. The CD signals at 282 and 255 nm show the same profile. The assays were performed in duplicate.

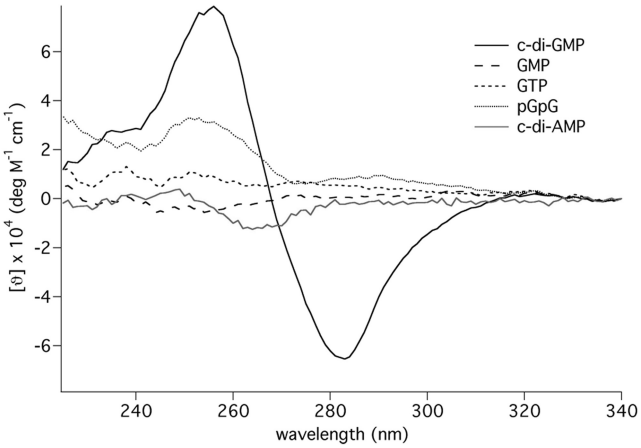

Figure 5. CD spectra of the nucleotides involved in c-di-GMP turnover. The nucleotides were analyzed at the concentration of 15 μM at 10°C in 50 mM Tris–HCl, pH 7.5, 150 mM NaCl, 10 mM $MgCl_2$ and 2.5 mM $MnCl_2$. The spectrum of cyclic-di-AMP is also shown to compare the behavior of the two cyclic dinucleotides (c-di-GMP and c-di-AMP).

if needed, also in the presence of Mg^{2+} ions alone (using a consistent calibration curve).

Interestingly, we have also observed that, in the presence of the diguanylate cyclase PleD, the CD signal of c-di-GMP increases even in absence of manganese in the buffer (Figure 7, black circles). This is because of c-di-GMP binding to the enzyme inhibitory site as an intercalated dimer (14) with a similar structure of the c-di-GMP–Mn^{2+} complex (Figure 3). Accordingly, titrating PleD with c-di-GMP, the CD signal increases linearly with c-di-GMP concentration until all the inhibitory sites of PleD are saturated (i.e. a PleD:c-di-GMP binding stoichiometry of 1:2) (Figure 7). Further addition of c-di-GMP does not correspond to a significant increase of the signal given that, in the absence of free binding sites, c-di-GMP is prevalently monomeric. Addition of manganese to the solution results in a further increase in the intensity of the signal, which indicates a shift of the equilibrium of free c-di-GMP towards the dimeric form (Figure 7, blue triangles). This result confirms that a sigmoidal CD spectra peaking at 255 and 282 nm can be regarded as the spectroscopic fingerprint of the intercalated dimer.

CONCLUSIONS

The method presented here is based on the specific CD signal displayed by the intercalated dimer of c-di-GMP and on the ability of manganese ions to promote dimerization of this cyclic dinucleotide. We have observed that c-di-GMP displays a sigmoidal CD signature, related to the formation of an intercalated dimer, which is enhanced in the presence of Mn^{2+}, but not Mg^{2+} ions. The crystallographic structure of the complex of c-di-GMP with Mn^{2+} clearly shows that c-di-GMP binds to the two metals with the same geometry; thus, our results suggest

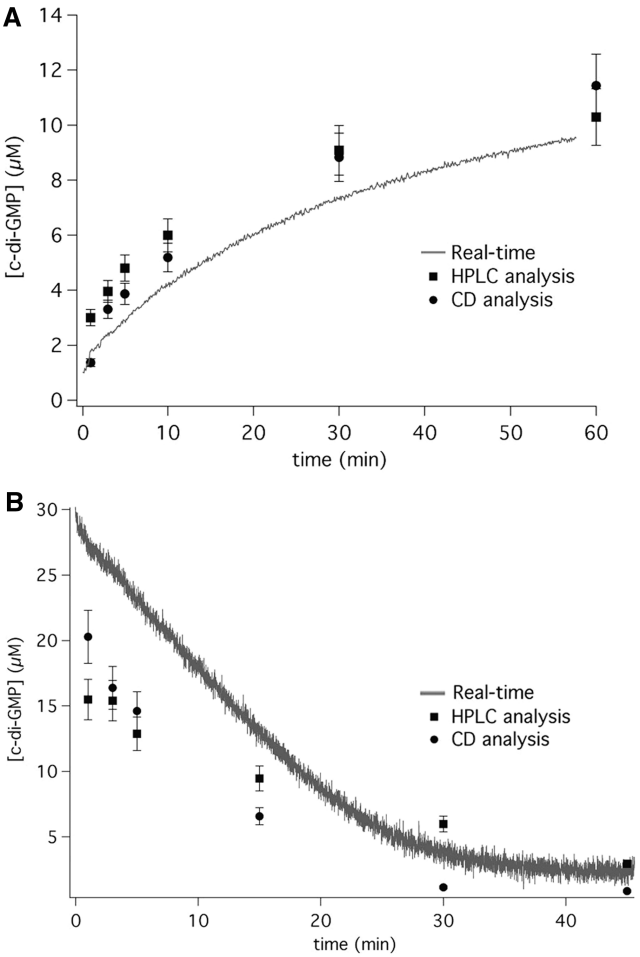

Figure 6. Time course of the reaction catalyzed by the diguanylate cyclase PleD (Panel **A**) and by the phosphodiesterase RocR (Panel **B**) as monitored in real-time by following the CD signal at 282 nm at 20°C (continuous line). As a control, the concentration of c-di-GMP in individual samples taken at given times during the reaction was determined separately by CD spectroscopy (black circles) and reverse-phase HPLC (black squares). The diguanylate cyclase activity of PleD (0.5 μM) was monitored using 100 μM GTP (Panel A) in 20 mM Tris, pH 8, 100 mM NaCl, 10 mM $MgCl_2$, 2.5 mM $MnCl_2$, 1 mM $BeCl_2$ and 10 mM NaF. The phosphodiesterase activity of RocR (0.5 μM) was monitored using 30 μM c-di-GMP (Panel B) in 20 mM Tris, pH 8, 100 mM NaCl, 5 mM $MgCl_2$ and 2.5 mM $MnCl_2$. All assays were performed in duplicate.

that the two divalent cations display a different ability to populate the complex in solution. The present method can be used to measure the enzymatic rate of c-di-GMP production and degradation, as shown by the real-time measurements carried out on two reference enzymes, i.e. PleD diguanylate cyclase and RocR phosphodiesterase. The CD signal of c-di-GMP at 282 nm is specific of the dimeric form of the molecule; other nucleotides, such as GTP, pGpG or GMP, which are present during the reaction of diguanylate cyclases or phosphodiesterases, do not show the same signal. Moreover, the observation that the adenine dinucleotide c-di-AMP does not have the same spectroscopic signature suggests that the sigmoidal CD signal can be assigned to the stacking of the guanine bases.

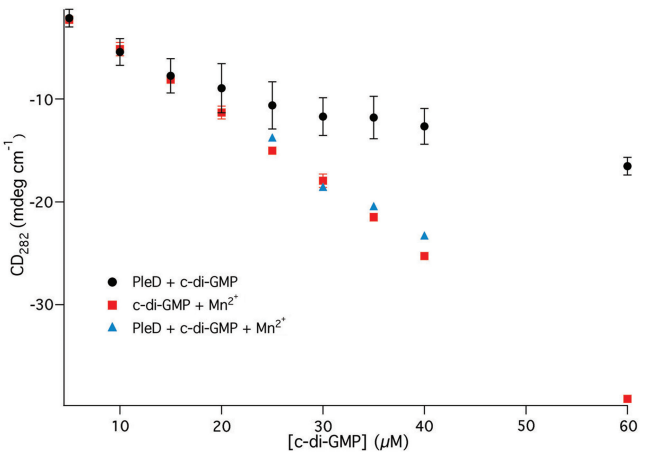

Figure 7. Plot of the CD signal at 282 nm of samples containing increasing amounts of c-di-GMP in the presence of 10 μM PleD (monomer) (circles) or 2.5 mM $MnCl_2$ (squares). Addition of 2.5 mM $MnCl_2$ to the samples containing 25, 30, 35 and 40 μM c-di-GMP and 10 μM PleD yields the same CD signal (triangles) of the manganese-alone samples. Experimental conditions were as follows: 20 mM Tris–HCl, pH 8, 100 mM NaCl, 10 mM $MgCl_2$, 1 mM $BeCl_2$ and 10 mM NaF. The assays were performed in triplicate.

Comparison of the distinctive features of the present method with those of the other methods available to measure enzymatic activities (as summarized in Table 1) underlines that this method is effective to measure steady-state kinetics of both DGCs and PDEs in real-time. As shown in Table 1, the kinetic properties of few enzymes have been studied to date with the methods already available; on the other hand, it is clear that a deep understanding of the mechanism controlling the turnover of c-di-GMP requires the biochemistry of its synthesis and degradation to be fully elucidated. A clear advantage of the approach presented here is that it allows to detect and to quantify c-di-GMP directly, without the need of additional chromophores, biosensors or dyes, and it does not require time-consuming sample preparation. In common with most methods, the sensitivity of the CD analysis lies in the micromolar range of c-di-GMP concentrations (Table 1). As far as real-time measurements are concerned, only the indirect EnzCheck method is suited to measure the time course of DGCs in real-time, but this method cannot be applied to PDEs; on the other hand, the activity of PDEs can be followed using the fluorescent MANT-c-di-GMP derivative as proposed by Sharma *et al.* (35).

In our opinion, the present experimental approach also opens novel scenarios and attractive possibilities in the field of c-di-GMP enzymes. The method will allow to conceive pre-steady state kinetic experiments, to date unexplored for these enzymes, but of crucial value to determine the reaction mechanism of both DGCs and PDEs. A detailed knowledge of the mechanistic details of these reactions is a necessary pre-requisite to design and to validate effective inhibitors that could be used as antimicrobial agents able to modulate c-di-GMP levels and to interfere with the formation of biofilms or with development of specific (antibiotic-resistant) phenotypes, such

as those found in persister cells (46). Moreover, the experimental approach presented here might be used to explore the interplay of DGCs and PDEs in controlling c-di-GMP levels by allowing to measure the activity of these enzymes not only individually but also in combination in the same reaction mixture; this may provide quantitative evaluation of the interaction of proteins putatively involved in the same signaling pathway. As suggested by the recent evaluation of the different phenotypic output of the activity of the DGCs in *Vibrio cholerae*, the mechanism and rate whereby each individual DGC produces c-di-GMP and/or is regulated determine the stringent biological specificity of c-di-GMP signaling in the cell (47).

ACCESSION NUMBERS

Structure of the c-di-GMP/Manganese complex (CCDC 913765).

SUPPLEMENTARY DATA

Supplementary Data are available at NAR Online: Supplementary Table 1, Supplementary Figures 1 and 2 and Supplementary Movie 1.

ACKNOWLEDGEMENTS

The authors wish to thank Manuela Caruso (Rome, I) for skilful technical assistance. The plasmid expressing the RocR gene is a kind gift of H. Sondermann (USA). A.B. acknowledges support from Deutscher Akademischer Auslandsdienst (DAAD) and Konrad-Adenauer-Stiftung.

FUNDING

Ministero della Università e Ricerca of Italy [RBRN07BMCT and 20094BJ9R7 to F.C, RBFR10LHD1 to S.R.]; Sapienza University of Rome; Fondazione Italiana Fibrosi Cistica [13/2009- with the contribution of Delegazione Novara and Delegazione Cosenza2 to F.C.]. Funding for open access charge: Ministero della Università e Ricerca of Italy.

Conflict of interest statement. None declared.

REFERENCES

1. Jenal,U. and Malone,J. (2006) Mechanisms of cyclic-di-GMP signaling in bacteria. *Annu. Rev. Genet.*, **40**, 385–407.
2. Hengge,R. (2009) Principles of c-di-GMP signalling in bacteria. *Nat. Rev. Microbiol.*, **7**, 263–273.
3. Ryan,R.P., Tolker-Nielsen,T. and Dow,J.M. (2012) When the PilZ don't work: effectors for cyclic di-GMP action in bacteria. *Trends Microbiol.*, **20**, 235–242.
4. Zhang,Z., Gaffney,B.L. and Jones,R.A. (2004) c-di-GMP displays a monovalent metal ion-dependent polymorphism. *J. Am. Chem. Soc.*, **126**, 16700–16701.
5. Zhang,Z., Kim,S., Gaffney,B.L. and Jones,R.A. (2006) Polymorphism of the signaling molecule c-di-GMP. *J. Am. Chem. Soc.*, **128**, 7015–7024.
6. Gentner,M., Allan,M.G., Zaehringer,F., Schirmer,T. and Grzesiek,S. (2012) Oligomer Formation of the bacterial second messenger c-di-GMP: reaction rates and equilibrium constants indicate a monomeric state at physiological concentrations. *J. Am. Chem. Soc.*, **134**, 1019–1029.
7. Nakayama,S., Kelsey,I., Wang,J., Roelofs,K., Stefane,B., Luo,Y., Lee,V.T. and Sintim,H.O. (2011) Thiazole orange-induced c-di-GMP quadruplex formation facilitates a simple fluorescent detection of this ubiquitous biofilm regulating molecule. *J. Am. Chem. Soc.*, **133**, 4856–4864.
8. Nakayama,S., Kelsey,I., Wang,J. and Sintim,H.O. (2011) c-di-GMP can form remarkably stable G-quadruplexes at physiological conditions in the presence of some planar intercalators. *Chem. Commun.*, **47**, 4766–4768.
9. Ko,J., Ryu,K.S., Kim,H., Shin,J.S., Lee,J.O., Cheong,C. and Choi,B.S. (2010) Structure of PP4397 reveals the molecular basis for different c-di-GMP binding modes by Pilz domain proteins. *J. Mol. Biol.*, **398**, 97–110.
10. Benach,J., Swaminathan,S.S., Tamayo,R., Handelman,S.K., Folta-Stogniew,E., Ramos,J.E., Forouhar,F., Neely,H., Seetharaman,J., Camilli,A. *et al.* (2007) The structural basis of cyclic diguanylate signal transduction by PilZ domains. *EMBO J.*, **26**, 5153–5166.
11. Duvel,J., Bertinetti,D., Moller,S., Schwede,F., Morr,M., Wissing,J., Radamm,L., Zimmermann,B., Genieser,H.G., Jansch,L. *et al.* (2012) A chemical proteomics approach to identify c-di-GMP binding proteins in *Pseudomonas aeruginosa*. *J. Microbiol. Methods*, **88**, 229–236.
12. Yang,C.Y., Chin,K.H., Chuah,M.L., Liang,Z.X., Wang,A.H. and Chou,S.H. (2011) The structure and inhibition of a GGDEF diguanylate cyclase complexed with (c-di-GMP)(2) at the active site. *Acta Crystallogr. D Biol. Crystallogr.*, **67**, 997–1008.
13. De,N., Pirruccello,M., Krasteva,P.V., Bae,N., Raghavan,R.V. and Sondermann,H. (2008) Phosphorylation-independent regulation of the diguanylate cyclase WspR. *PLoS Biol.*, **6**, e67.
14. Chan,C., Paul,R., Samoray,D., Amiot,N.C., Giese,B., Jenal,U. and Schirmer,T. (2004) Structural basis of activity and allosteric control of diguanylate cyclase. *Proc. Natl Acad. Sci. USA*, **101**, 17084–17089.
15. Minasov,G., Padavattan,S., Shuvalova,L., Brunzelle,J.S., Miller,D.J., Basle,A., Massa,C., Collart,F.R., Schirmer,T. and Anderson,W.F. (2009) Crystal structures of YkuI and its complex with second messenger cyclic Di-GMP suggest catalytic mechanism of phosphodiester bond cleavage by EAL domains. *J. Biol. Chem.*, **284**, 13174–13184.
16. Navarro,M.V., De,N., Bae,N., Wang,Q. and Sondermann,H. (2009) Structural analysis of the GGDEF-EAL domain-containing c-di-GMP receptor FimX. *Structure*, **17**, 1104–1116.
17. Wang,J., Zhou,J., Donaldson,G.P., Nakayama,S., Yan,L., Lam,Y.F., Lee,V.T. and Sintim,H.O. (2011) Conservative change to the phosphate moiety of cyclic diguanylic monophosphate remarkably affects its polymorphism and ability to bind DGC, PDE, and PilZ proteins. *J. Am. Chem. Soc.*, **133**, 9320–9330.
18. Paul,R., Weiser,S., Amiot,N.C., Chan,C., Schirmer,T., Giese,B. and Jenal,U. (2004) Cell cycle-dependent dynamic localization of a bacterial response regulator with a novel di-guanylate cyclase output domain. *Genes Dev.*, **18**, 715–727.
19. Paul,R., Abel,S., Wassmann,P., Beck,A., Heerklotz,H. and Jenal,U. (2007) Activation of the diguanylate cyclase PleD by phosphorylation-mediated dimerization. *J. Biol. Chem.*, **282**, 29170–29177.
20. Christen,B., Christen,M., Paul,R., Schmid,F., Folcher,M., Jenoe,P., Meuwly,M. and Jenal,U. (2006) Allosteric control of cyclic di-GMP signaling. *J. Biol. Chem.*, **281**, 32015–32024.
21. Tuckerman,J.R., Gonzalez,G., Sousa,E.H., Wan,X., Saito,J.A., Alam,M. and Gilles-Gonzalez,M.A. (2009) An oxygen-sensing diguanylate cyclase and phosphodiesterase couple for c-di-GMP control. *Biochemistry*, **48**, 9764–9774.
22. Neunuebel,M.R. and Golden,J.W. (2008) The Anabaena sp. strain PCC 7120 gene all2874 encodes a diguanylate cyclase and is required for normal heterocyst development under high-light growth conditions. *J. Bacteriol.*, **190**, 6829–6836.
23. Christen,M., Christen,B., Folcher,M., Schauerte,A. and Jenal,U. (2005) Identification and characterization of a cyclic di-GMP-specific phosphodiesterase and its allosteric control by GTP. *J. Biol. Chem.*, **280**, 30829–30837.

24. Sultan,S.Z., Pitzer,J.E., Boquoi,T., Hobbs,G., Miller,M.R. and Motaleb,M.A. (2011) Analysis of the HD-GYP domain cyclic dimeric GMP phosphodiesterase reveals a role in motility and the enzootic life cycle of *Borrelia burgdorferi*. *Infect. Immun.*, **79**, 3273–3283.
25. Wassmann,P., Chan,C., Paul,R., Beck,A., Heerklotz,H., Jenal,U. and Schirmer,T. (2007) Structure of BeF3- -modified response regulator PleD: implications for diguanylate cyclase activation, catalysis, and feedback inhibition. *Structure*, **15**, 915–927.
26. Lai,T.H., Kumagai,Y., Hyodo,M., Hayakawa,Y. and Rikihisa,Y. (2009) The *Anaplasma phagocytophilum* PleC histidine kinase and PleD diguanylate cyclase two-component system and role of cyclic Di-GMP in host cell infection. *J. Bacteriol.*, **191**, 693–700.
27. Sawai,H., Yoshioka,S., Uchida,T., Hyodo,M., Hayakawa,Y., Ishimori,K. and Aono,S. (2010) Molecular oxygen regulates the enzymatic activity of a heme-containing diguanylate cyclase (HemDGC) for the synthesis of cyclic di-GMP. *Biochim. Biophys. Acta*, **1804**, 166–172.
28. Rao,F., Pasunooti,S., Ng,Y., Zhuo,W., Lim,L., Liu,A.W. and Liang,Z.X. (2009) Enzymatic synthesis of c-di-GMP using a thermophilic diguanylate cyclase. *Anal. Biochem.*, **389**, 138–142.
29. He,Y.W., Boon,C., Zhou,L. and Zhang,L.H. (2009) Co-regulation of *Xanthomonas campestris* virulence by quorum sensing and a novel two-component regulatory system RavS/RavR. *Mol. Microbiol.*, **71**, 1464–1476.
30. Rao,F., Yang,Y., Qi,Y. and Liang,Z.X. (2008) Catalytic mechanism of cyclic di-GMP-specific phosphodiesterase: a study of the EAL domain-containing RocR from *Pseudomonas aeruginosa*. *J. Bacteriol.*, **190**, 3622–3631.
31. Barends,T.R., Hartmann,E., Griese,J.J., Beitlich,T., Kirienko,N.V., Ryjenkov,D.A., Reinstein,J., Shoeman,R.L., Gomelsky,M. and Schlichting,I. (2009) Structure and mechanism of a bacterial light-regulated cyclic nucleotide phosphodiesterase. *Nature*, **459**, 1015–1018.
32. Rao,F., Qi,Y., Chong,H.S., Kotaka,M., Li,B., Li,J., Lescar,J., Tang,K. and Liang,Z.X. (2009) The functional role of a conserved loop in EAL domain-based cyclic di-GMP-specific phosphodiesterase. *J. Bacteriol.*, **191**, 4722–4731.
33. Yang,F., Tian,F., Sun,L., Chen,H., Wu,M., Yang,C.H. and He,C. (2012) A novel two-component system PdeK/PdeR regulates c-di-GMP turnover and virulence of *Xanthomonas oryzae* pv. oryzae. *Mol. Plant Microbe Interact.*, **25**, 1361–1369.
34. Ryan,R.P., Fouhy,Y., Lucey,J.F., Crossman,L.C., Spiro,S., He,Y.W., Zhang,L.H., Heeb,S., Cámara,M., Williams,P. *et al.* (2006) Cell-cell signaling in *Xanthomonas campestris* involves an HD-GYP domain protein that functions in cyclic di-GMP turnover. *Proc. Natl Acad. Sci. USA*, **103**, 6712–6717.
35. Sharma,I.M., Dhanaraman,T., Mathew,R. and Chatterji,D. (2012) Synthesis and Characterization of a fluorescent analogue of cyclic di-GMP. *Biochemistry*, **51**, 5443.
36. Egli,M., Gessner,R.V., Williams,L.D., Quigley,G.J., van der Marel,G.A., van Boom,J.H., Rich,A. and Frederick,C.A. (1990) Atomic-resolution structure of the cellulose synthase regulator cyclic diguanylic acid. *Proc. Natl Acad. Sci. USA*, **87**, 3235–3239.
37. Altomare,A., Burla,M.C., Camalli,M., Cascarano,G., Giacovazzo,C., Guagliardi,A., Moliterni,A.G.G., Polidori,G. and Spagna,R. (1999) Sir97: a new tool for crystal structure determination and refinement. *J. Appl. Crystallogr.*, **32**, 115–119.
38. Sheldrick,G.M. (2008) A short history of SHELX. *Acta Crystallogr. A*, **64**, 112–122.
39. Kelly,S.M. and Price,N.C. (2000) The use of circular dichroism in the investigation of protein structure and function. *Curr. Protein Pept. Sci.*, **1**, 349–384.
40. Liaw,Y.C., Gao,Y.G., Robinson,H., Sheldrick,G.M., Sliedregt,L.A., van der Marel,G.A., van Boom,J.H. and Wang,A.H. (1990) Cyclic diguanylic acid behaves as a host molecule for planar intercalators. *FEBS Lett.*, **264**, 223–227.
41. Zhang,Y. and Huang,K. (2007) On the interactions of hydrated metal cations (Mg2+, Mn2+, Ni2+, Zn2+) with guanine–cytosine Watson–Crick and guanine–guanine reverse-Hoogsteen DNA base pairs. *J. Mol. Struct. THEOCHEM*, **812**, 51–62.
42. Eichhorn,G.L. and Shin,Y.A. (1968) Interaction of metal ions with polynucleotides and related compounds: part XII. The relative effect of various metal ions on DNA helicity. *J. Am. Chem. Soc.*, **90**, 7323–7328.
43. Solt,I., Simon,I., Csaszar,A.G. and Fuxreiter,M. (2007) Electrostatic versus nonelectrostatic effects in DNA sequence discrimination by divalent ions Mg2+ and Mn2+. *J. Phys. Chem. B*, **111**, 6272–6279.
44. Sponer,J.E., Sychrovsky,V., Hobza,P. and Sponer,J. (2004) Interactions of hydrated divalent metal cations with nucleic acid bases. How to relate the gas phase data to solution situation and binding selectivity in nucleic acids. *Phys. Chem. Chem. Phys.*, **6**, 2772–2780.
45. Antoniani,D., Bocci,P., Maciag,A., Raffaelli,N. and Landini,P. (2009) Monitoring of diguanylate cyclase activity and of cyclic-di-GMP biosynthesis by whole-cell assays suitable for high-throughput screening of biofilm inhibitors. *Appl. Microbiol. Biotechnol.*, **85**, 1095–1104.
46. Malone,J.G., Jaeger,T., Manfredi,P., Dötsch,A., Blanka,A., Bos,R., Cornelis,G.R., Häussler,S. and Jenal,U. (2012) The YfiBNR signal transduction mechanism reveals novel targets for the evolution of persistent *Pseudomonas aeruginosa* in cystic fibrosis airways. *PLoS Pathog.*, **8**, e1002760.
47. Massie,J.P., Reynolds,E.L., Koestler,B.J., Cong,J.P., Agostoni,M. and Waters,C.M. (2012) Quantification of high-specificity cyclic diguanylate signaling. *Proc. Natl Acad. Sci. USA*, **109**, 12746–12751.